This paper is available on line at http://www.mcponline.org

Pharmacoproteomic Analysis of a Novel Cell-permeable Peptide Inhibitor of Tumor-induced Angiogenesis*

Ji-Young Bang‡, Eung-Yoon Kim‡, Dong-Ku Kang‖, Soo-Ik Chang**, Moon-Hi Han‡‡, Kwang-Hyun Baek§§, and In-Cheol Kang‡§¶¶¶

P11, a novel peptide ligand containing a PDZ-binding motif (Ser-Asp-Val) with high affinity to integrin $\alpha_v\beta_3$ was identified from a hexapeptide library (PS-SPCL) using a protein microarray chip-based screening system. Here, we investigated the inhibitory mechanism of P11 (HSDVHK) on tumor-induced angiogenesis via a pharmacoproteomic approach. P11 was rapidly internalized by , human umbilical vein endothelial cells (HUVECs) via an integrin $\alpha_v\beta_3$-mediated event. Caveolin and clathrin appeared to be involved in the P11 uptake process. The cell-penetrating P11 resulted in suppression of bFGF-induced HUVEC proliferation in a dose-dependent manner. Phosphorylation of extracellular-signal regulated kinase (ERK1/2) and mitogen-activated protein kinase kinase (MEK) in bFGF-stimulated HUVECs was inhibited by cell-permeable P11. Proteomic analysis via antibody microarray showed up-regulation of p53 in P11-treated HUVECs, resulting in induction of apoptosis via activation of caspases-3, -8, and -9. Several lines of experimental evidence strongly suggest that the molecular mechanism of P11, a novel anti-angiogenic agent, inhibits bFGF-induced HUVEC proliferation via mitogen-activated protein kinase kinase and extracellular-signal regulated kinase inhibition as well as p53-mediated apoptosis related with activation of caspases. ***Molecular & Cellular Proteomics 10: 10.1074/mcp.M110.005264, 1–11, 2011.***

Angiogenesis occurs through the outgrowth of new capillaries from pre-existing blood vessels and involves degradation of the extracellular matrix (ECM)[1] as well as migration, proliferation and differentiation of endothelial cells into tubular networks (1). Angiogenesis can be stimulated by various positive factors such as fibroblast growth factors (FGFs), transforming growth factor β, tumor necrosis factor-α, vascular endothelial growth factor, and angiogenin (2, 3), among others. The expression of integrin $\alpha_v\beta_3$ on vascular endothelial cells in human tumors is markedly up-regulated by several growth factors *in vitro*. Therefore, antibodies or peptides capable of blocking the activity of integrin $\alpha_v\beta_3$ are classified as anti-angiogenic (4–8). In this vein, several reports suggest that integrin $\alpha_v\beta_3$ is a target for anti-angiogenic therapy (7–10). Several growth factors including FGF2 and tumor necrosis factor-α increase $\alpha_v\beta_3$ expression in the developing blood vessels of chick embryo (11) and rabbit cornea (5). $\alpha_v\beta_3$ expression is also stimulated by human tumors cultured on chick chorioallantoic membrane, rabbit cornea, and SCID mice (12). Antagonists of $\alpha_v\beta_3$, including Arg-Gly-Asp(RGD)-containing disintegrins, cyclic RGD peptides, and monoclonal antibodies, significantly suppress cytokine- and solid tumor fragment-stimulated angiogenesis in proliferating vascular endothelial cells by inducing apoptosis (11, 6). Thus, $\alpha_v\beta_3$ is a suitable target for the prevention of angiogenesis induced by tumors. Cell-permeable peptides such as RGD peptide promote apoptosis of T lymphocytes and, human umbilical vein endothelial cells (HUVECs) by causing conformational changes that lead to the activation of caspases-3, -8 and -9 (13, 14). RGD peptides perform pro-apoptotic functions in angiogenesis, inflammation, and metastasis (15–18).

Pharmacoproteomic analysis allows us to investigate the modes of action of new drug molecules in biological samples. The present study demonstrates via a proteomic approach based on antibody microarray that P11, a hexapeptide (HSDVHK) containing a novel integrin-binding motif, SDV (a Type I PDZ-binding motif), prevented tumor-induced new blood vessel formation and growth of subcutaneous solid tumors. We found that the anti-angiogenic properties of P11 were due to its ability to specifically target $\alpha_v\beta_3$ and penetrate HUVECs, resulting in the suppression of bFGF-induced HUVEC proliferation in endothelial cells via perturbation of mitogen-acti-

From the Address: ‡InnoPharmaScreen Inc.; §Department of Biological Science, College of Natural Science; ¶BioChip Research Center, and Hoseo University, Asan 336-795, Korea; ‖Department of Chemistry, Imperial College London, South Kensington, SW7 2AZ, UK; **Department of Biochemistry, College of Natural Science, Chungbuk National University, Cheongju 361-763, Korea; ‡‡Proteogen, Inc., RM 1516 Windstone Officetel, #275-2 Yangjae-dong, Seocho-ku, Seoul 137-130, Korea; §§Department of Biomedical Science, CHA University, Seoul 135-081, Korea

Received October 1, 2010, and in revised form, March 1, 2011

Published, MCP Papers in Press, May 10, 2011, DOI 10.1074/mcp.M110.005264

[1] The abbreviations used are: ECM, extracellular matrix; FGF, fibroblast growth factor; HUVEC, human umbilical vein endothelial cells; PBS, phosphate-buffered saline; TUNEL, transferase-mediated dUTP nick end labeling.

vated protein kinase kinase (MEK) and extracellular signal-regulated kinase (ERK)1/2 signaling and p53-mediated induction of apoptosis.

EXPERIMENTAL PROCEDURES

Reagents—Integrin $\alpha_v\beta_3$ and vitronectin were purchased from Chemicon International Inc. (Temecula, CA). HUVECs and M199 (Invitrogen), Penicillin-Streptomycin (10,000 IU/ml; Invitrogen), 25 mM HEPES, 10 units/ml of Heparin, 2.2 g/L of sodium bicarbonate, 20% fetal bovine serum (FBS) and 20 ng/ml of bFGF were from Innopharmascreen Inc. (Asan, Korea). Protease inhibitor mixture was from Roche Applied Science (Indianapolis, IN) and DC protein assay kit II was from Bio-Rad (Hercules, CA). Mouse anti-human/mouse β-actin (A5316) was from Sigma Chemical. Goat anti-mouse IgG HRP conjugated secondary antibody was from Zymed Laboratories (San Francisco, CA) and goat anti-rabbit IgG HRP conjugated secondary antibody was from Pierce (Rockford, IL). FITC or TRITC-conjugated secondary antibody and DAPI were purchased from Sigma. Antibodies against α5, α_v integrin, and clathrin were from Chemicon (Temecula, CA); antibody against caveolin was from Upstake (NY, USA). Casapase colorimetric assay kit and *in situ* cell death detection kit were from R&D (Minneapolis, MN) and Roche, respectively. RGD, RGE peptides, and FITC-labeled P11 were from Peptron (Daejeon, KOREA). 4× NuPAGE LDS sample buffer, 4–12% NuPAGE Bis-Tris gels and NuPAGE MES SDS running buffer were from Invitrogen (Carlsbad, CA). Hybond ECL transfer membrane and ECL Western blotting detection kit were from Amercham Pharmacia (Arlington Heights, IL). X-ray films were from Agfa-Gevaert (CP-BU, N. V., Belgium). ProteoChip was from Proteogen Inc. (Seoul, Korea). All peptides used in this study were synthesized by Peptron Inc. (Taejeon, Korea).

Cell Culture—HUVECs were maintained in a mixture of M199 (Invitrogen), Penicillin-Streptomycin (10,000 IU/ml; Invitrogen), 25 mM HEPES, 10 units/ml of Heparin, 2.2g/L of sodium bicarbonate, 20% FBS, and 20 ng/ml of bFGF were from Innopharmascreen Inc. (Asan, Korea). Cells at passages 3 to 6 were used. HUVEC cultures were kept at 37 °C in a humidified atmosphere of 5% CO_2 in air.

Protein Expression Profiles in P11-Treated HUVECs Using an Antibody Microarray Chip—Forty-eight individual antibodies against proteins involved in the cell cycle were spotted onto a ProteoChip (Proteogen Inc. Korea) in duplicate. Capture proteins (antibodies) were diluted to a working concentration of 100 μg/ml in phosphate-buffered saline (PBS) containing 20% PEG, and microspots of capture proteins were developed at 37 °C for 3 h. The chip was then washed, blocked (blocking buffer: 3% bovine serum albumin, 0.5% Tween-20 in PBS) for 1 h on a shaker at room temperature, washed again with PBST (PBS containing 0.2% Tween 20) to remove excess BSA and then dried under a stream of N_2 gas. The fluorescence-labeled cell lysates (1 mg/ml) were applied to the spots of capture proteins, followed by incubation for 1 h at 37 °C. The slides were washed three times with PBST, N_2-dried and analyzed using a fluorescence microarray scanner (Axon Instruments, Foster City, CA). The ratios of Cy5 to Cy3 for each spot were calculated using the manufacturer's software package (Genepix 6.0, Axon Instruments), and all experiments were repeated at least three times.

The microarray analysis was conducted using the Genepix software package. The slides were first scanned at the optimal conditions for each individual slide, and data were reviewed as a scatter plot of Cy5 *versus* Cy3 intensities. The replicate values within each slide were signal intensities. Cy5 to Cy3 ratios were calculated by Internally Normalized Ratios method using Microsoft® Excel. The average median ratio values for the spots were normalized to 1.0, which represents unchanged protein expression. Each data point presented in this report represents the average of at least three experiments. Average values (normalized Cy5/Cy3 ratios) were sorted by differences in expression.

Internalization of P11 into HUVECs—HUVECs (6×10^4) were plated on coverslips coated with denatured collagen, and left for 16 h in a CO_2 incubator. The cells were treated with FITC-labeled P11 (10 ng/ml) at 4 °C or 37 °C for various times. NIH3T3 cells were plated on coverglass slides in Dulbecco's modified Eagle's medium at a density of 70,000 cells/well, with each slide laying separately at the base of each well in a 6-well plate. After overnight attachment, the cells were incubated for 1 min, 5 min, 20 min, or 1 h, at 37 °C with 1 μg/ml of FITC-conjugated P11. HUVECs and NIH 3T3 cells were then viewed and photographed by a Leica confocal microscope using a FITC filter.

In Vitro bFGF-Induced HUVEC Proliferation—HUVECs (8000 cells per well) in M199 containing Penicillin-Streptomycin (10,000 IU/ml), 25 mM HEPES, 10 units/ml of Heparin, 2.2g/L of sodium bicarbonate, 20% fetal bovine serum, and 20 ng/ml of bFGF were plated onto 24-well tissue culture plates coated with denatured collagen. NIH 3T3 cells and U87 glioma cells (70,000 cells per well) were plated on 24-well plates in DMEM containing 10% fetal calf serum. After 24 h, the media were replaced with a serum-depleted medium containing 2% fetal calf serum for 2 h, after which each sample was added to the cells in triplicate. After 48 h, adherent cells were dispersed in trypsin and counted. Data presented are from triplicate.

Determination of Activity of Caspase-3, Caspase-8, and Caspase-9—The enzyme activities of caspases-3, -8, and -9 were measured in cells using kits purchased from R&D. P11-treated and -untreated cells were homogenized in cell lysis buffer, and the homogenates were centrifuged at 10,000 × *g* for 5 min at 4 °C in a microcentrifuge. Using the 96-well plate microassay method, the activity levels of caspases-3, -8, and -9 were analyzed in the supernatants. Supernatants (50 μg) from each test sample were incubated in a final volume of 100 μl for 60 min at 37 °C in a working solution containing DEVD-pNA (a synthetic caspase-3 substrate), IETD-pNA(a synthetic caspase-8 substrate), or LEHD-pNA (a synthetic caspase-9 substrate). The absorbance was read at 405 nm by an ELISA plate reader after 60 min. Caspase activity was calculated as micromoles per gram of cells using a p-nitroaniline calibration curve. The data were plotted as A405 *versus* time for each sample, and activity was calculated *versus* control cells. The experiments were repeated three times.

In Situ Terminal Deoxynucleotidyl Transferase-mediated dUTP Nick End Labeling (TUNEL) Assay—A TUNEL apoptosis detection kit (Roche) was used for DNA fragmentation fluorescence staining according to the manufacturer's protocol. Briefly, HUVECs were cocultured with FITC-labeled P11. Cells were fixed for 24 h with 4% paraformaldehyde in 0.1 M phosphate buffer (pH 7.4) and then incubated with a reaction mix containing biotin-dUTP and terminal deoxynucleotidyl transferase for 60 min. Positively stained fluorescein-labeled cells were visualized and photographed using fluorescence microscopy.

Transcription Factor Assay—Transcription factor assay was performed using a BD™ TransFactor profiling kit (BD Science) according to the manufacturer's instructions. In brief, Transfactor/blocking buffer was added to the wells (150 μl/well) and incubated for 15 min at room temperature. HUVECs were pretreated with P11 for 30 min, after which bFGF (3 ng/ml) was added to the cell medium. After 30 min, 30 μl of HUVEC lysates with Transfactor/blocking buffer were prepared. Buffer present in the wells was removed, and then cell lysates (50 μl) diluted with buffer were added to the wells. The plates were then incubated for 60 min at room temperature and washed three times with buffer. Primary antibodies against ATF-2, CREB-1, c-Fos, NF-kB (p65), NF-kB (p50), and c-Rel diluted with transfactor/blocking buffer were added to each well and then incubated for 60 min at room temperature. The plates were washed three times, after which secondary antibodies diluted with buffer were added to the

wells and incubated for 30 min at room temperature. The plates were again washed four times with Transfactor buffer (no blocking reagent) for 4 min. TMB substrate was then added to each well, followed by incubation for 10 min at room temperature. After a blue color had developed, the enzyme reaction was stopped by the addition of 100 ml of stop solution per well. The absorbance of the material in each plate was measured at 655 nm.

Immunostaining—HUVECs were fixed with 4% paraformaldehyde in PBS for 20 min, permeabilized with 0.25% Triton X-100 in PBS for 10 min, and then blocked with 1% bovine serum albumin in PBS for 30 min. Cells were stained with appropriate primary antibodies followed by FITC- or TRITC-conjugated secondary antibodies. To quantify intracellular fluorescence intensity, *z*-series confocal images and differential interference contrast images of cells were collected at the same time. The fluorescence intensity within individual cells was normalized by cell area. Immunofluorescence images of HUVECs were taken using a confocal laser scanning microscope (CLSM; Carl ZEISS, LSM 510 Meta, Jena, Germany).

Western Blot Analysis—HUVECs were cultured in M199 until 70% confluency and then grown in M199 supplemented with 1% fetal bovine serum for 16 h. The medium was replaced with fresh low serum medium with or without P11. After 30 min, bFGF (3 ng/ml) was added to the medium. At various time points, the cells were washed with PBS (HyClone, Logan, Utah), and cell lysates were prepared in lysis buffer (50 mM Tris-Cl, pH 7.5, 3.0 mM EGTA, 0.5% Triton X-100, 12 mM β-glycerophosphate, 150 mM sodium chloride, 50 mM sodium fluoride, 1.0 mM sodium vanadate, 2.0 mM dithiothreitol, 1.0 mM phenylmethylsulfonyl fluoride, 0.5 μg/ml of aprotinin, 0.1% β-mercaptoethanol and 1$\times$ protease inhibitor mixture). Cell lysates were clarified by centrifugation, and protein concentrations were determined using a DC protein assay kit. Lysates containing 50 μg of protein were loaded into each well and separated through NuPAGE™ 4~12% Bis-Tris gel (Invitrogen, Carlsbad, CA) electrophoresis. Gels were soaked in transfer buffer (25 mM Tris-HCl, 250 mM glycine, and 20% methanol), and proteins were then transferred to polyvinylidene difluoride membranes. Nonspecific binding sites were blocked by incubation with 5% nonfat dry milk in TBS-T (25 mM Tris-HCl, 137 mM NaCl, 137 mM KCl, 0.1% Tween 20, pH 7.4). The polyvinylidene difluoride membranes were then incubated with primary antibodies against MEK(1:1000), p-MEK(1:500), ERK1/2 (1:1000), pERK1/2 (1:500), p53(1:1,000), PCNA (1:1000), DMC1(1:500), or GAPDH (1:20,000) in TBS-T containing 3% nonfat dry milk at 4 °C overnight. Membranes were washed with TBS-T and incubated with secondary antibodies (1:3000). Signals were then developed using an ECL Western blotting detection kit and exposed to x-ray films.

RESULTS

Antiproliferation in P11-treated HUVECs—We identified P11 (HSDVHK), a novel peptide inhibitor of integrin $\alpha_v\beta_3$, via protein microarray of a hexapeptide library. P11 has been shown to inhibit the integrin $\alpha_v\beta_3$-vitronectin interaction in a dose-dependent manner (21). The SDV sequence of P11 is able to recognize the vitronectin-binding site (RGD-binding site) of integrin $\alpha_v\beta_3$ in a site-specific manner (22). To determine the antiangiogenic mechanism of P11 as an antagonist of integrin $\alpha_v\beta_3$, we first examined the effect of P11 on endothelial cell proliferation. Using an *in vitro* cell proliferation assay system, we found that P11 significantly inhibited HUVEC proliferation on denatured collagen-coated plates in a dose-dependent manner, whereas GRGDSP and HGLLHK inhibited cell proliferation poorly or not at all (Fig. 1*A*). The proliferation of NIH 3T3 cells and U87 leukemia cells was not affected by P11 treatment (Figs. 1*B* and 1*C*). The inhibitory efficacy of P11 was much higher than that of synthetic RGD peptide (GRGDSP). Half-maximal inhibition of cell proliferation was observed on denatured collagen-coated plates with ~12 μM P11, which corresponds to a concentration of 8 μg/ml. These data suggest that specific blocking of integrin $\alpha_v\beta_3$-mediated cellular signaling in response to HUVEC proliferation by P11 may result in the dose-dependent inhibition of cell proliferation.

Proteomic Analysis of Antiangiogenic Effect of P11 by Antibody Microarray—To investigate the possible mechanisms by which P11 mediates its antiangiogenic effect, we analyzed cell signaling protein expression profiles in P11-treated HUVECs by antibody microarray. To perform the protein profile analysis, cell lysates obtained from P11 and bFGF-treated HUVECs or bFGF-treated HUVECs were labeled with Cy3 or Cy5, respectively. The lysates were mixed and spotted on a prefabricated antibody microarray. The fluorescence intensities of the spots were measured using a fluorescence scanner, and the differential protein expression pattern between the two samples was then determined *A* (Fig. 2). To identify proteins that showed altered expression levels in response to P11, the distribution of fluorescence intensities (Cy3 and Cy5) for all of the spots was normalized with the mean values of the Cy5:Cy3 ratios of the protein spots. Using graded virtual images showing the Cy5:Cy3 ratios of the tested spots as well as normalized median values of the calculated Cy5:Cy3 ratios of the proteins, we could identify and select the changed protein spots (Figs. 2*A* and 2*B*). The normalized median of the ratio was used to represent the expression level of each protein. Protein expression measurements from the antibody microarrays were treated as independent observations. The normalized median of the Cy5:Cy3 ratio was calculated for each protein and graphically represented (Fig. 2*C*). Based on the data from three independent experiments, p53 was defined as up-regulated in P11-treated HUVECs, and there was no observation of down regulated proteins in cells after three independent experiments. The levels of all other proteins were unchanged according to the antibody microarray analysis (Fig. 2). We then performed an assay involving immunoblot analysis to validate the antibody microarray data. p53 was the only protein up-regulated with P11, as determined by Western blotting (Fig. 2*D*). This observation confirms that the Western blotting data are consistent with those obtained from the antibody microarray. It was reported that cyclic peptide inhibitors of integrin $\alpha_v\beta_3$ suppressed retinal angiogenesis in p53 wild-type mice, yet had no antiangiogenic activity in p53-deficient mice (23). These results strongly suggest that the specific up-regulation of p53 in response to HUVEC proliferation by P11 may result in the dose-dependent inhibition of the cell proliferation. In addition, the expression of MDM2, the principal cellular antagonist of p53, was decreased in P11-treated HUVECs compared with bFGF-induced control group (Fig. 2*E*). MDM2 is an E3 ubiquitin ligase and enhances p53

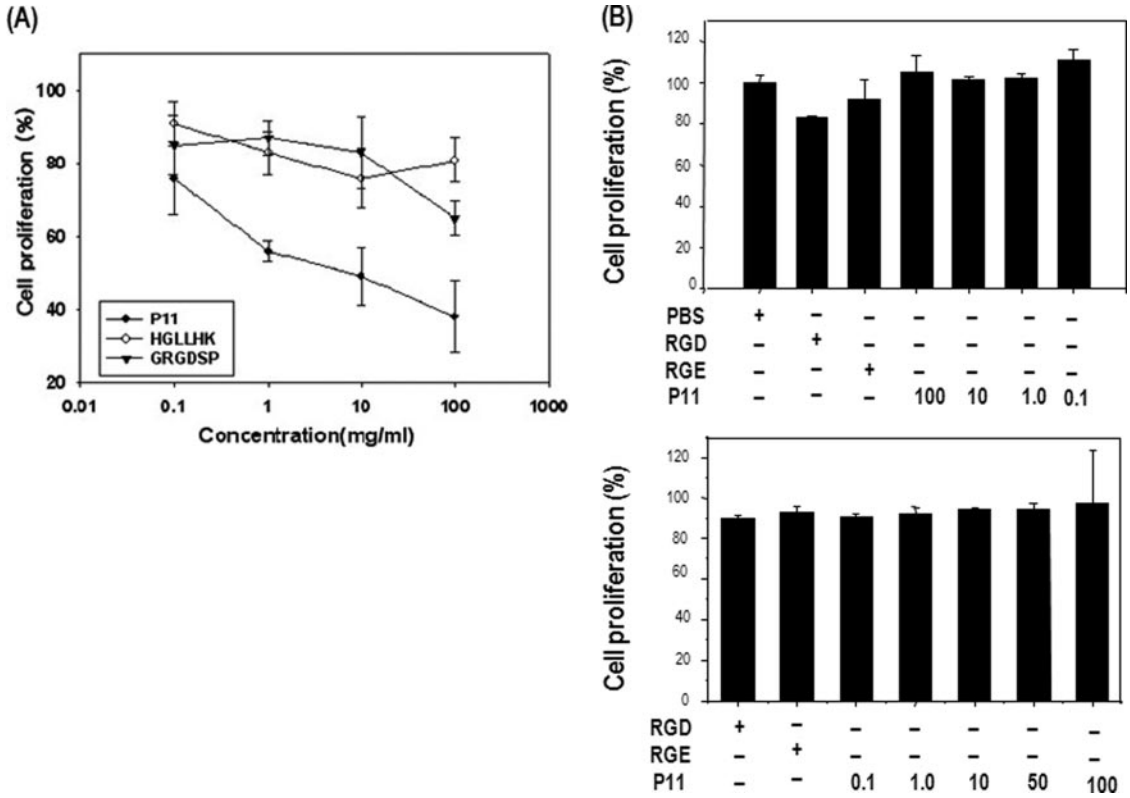

FIG. 1. **Inhibition of HUVEC proliferation by P11.** *A*, HUVECs were incubated with different concentrations (0.1, 1, 10, and 100 μg/ml) of P11 for 72 h. The adherent cells were then trypsinized and counted. *B*, and *C*, NIH 3T3 cells and U87 glioma cells were incubated with different concentrations (0.1, 1, 10, and 100 μg/ml) of P11, RGD peptide (500 μg/ml) or RGE peptide (500 μg/ml) for 48 h. The adherent cells were then trypsinized and counted.

degradation via an ubiquitin dependent pathway on nuclear and cytoplasmic 26S proteasomes in unstressed cells (24–28). The interaction between p53 and MDM2 is conformation-based and is tightly regulated on multiple levels. Disruption of the p53-MDM2 complex by multiple routes is the pivotal event for p53 activation, leading to p53 induction and its biological response (29). Thus, this finding indicates that the p53 up-regulation in HUVECs by treatment of P11 is closely related with down-regulation of MDM2 in terms of p53 stability.

Induction of Apoptosis in P11-treated HUVECs Via Activation of Caspases—It has been reported that several endogenous anti-angiogenic proteins such as endostatin, tumstatin and canstatin induce apoptosis in proliferating endothelial cells (18, 30–39).

Synthetic RGD peptide, a cell-permeable peptide, shows induction of apoptosis via activation of caspase 3, 8, and 9 in human endothelial cells (13, 14). Casepase-8, which plays a role in p53-induced apoptosis, was activated by unligated integrin $\alpha_v\beta_3$ followed by apoptosis (40). Inhibition of the caspase-9 death pathway could be important in pathological forms of angiogenesis, and correlations have been made between endothelial cell survival and expression or activity of p53 (23). To test whether or not the antiproliferative effect of P11 on bFGF-stimulated HUVECs is due to p53-induced apoptosis, we used a caspase activity assay and TUNEL assay. P11 remarkably increased the enzyme activities of caspases-3, -8, and -9 compared with bFGF-induced HUVECs (Fig. 3*A*). Apoptosis was observed in P11-treated HUVECs stimulated with bFGF through *in situ* apoptosis TUNEL assay (Fig. 3*B*). These findings suggest that the inhibition of HUVEC proliferation by P11 was due to the induction of HUVEC cell death through caspases activations and its mechanism was related with increased p53 expression.

Internalization of P11 into HUVECs—We next tried to determine how P11 inhibits angiogenesis in HUVECs by performing biochemical and cell-based assays. As it was reported that apoptosis of HUVECs is induced by internalization of RGD peptide (13, 14), we first tested if and how P11 can penetrate into HUVECs. We found that when P11 was administered into the culture media, HUVECs rapidly internalized the peptide in a time- and temperature-dependent manner. When the culture temperature was 37 °C, P11 rapidly penetrated into the cells, whereas at 4 °C, P11 was retained on the cell surface (Fig. 4*A*). In contrast, NIH 3T3 fibroblast cells did not internalize P11 regardless of temperature or time (data not shown). To assess whether or not P11 internalization is mediated by integrin $\alpha_v\beta_3$ present on the cell surface, we tested

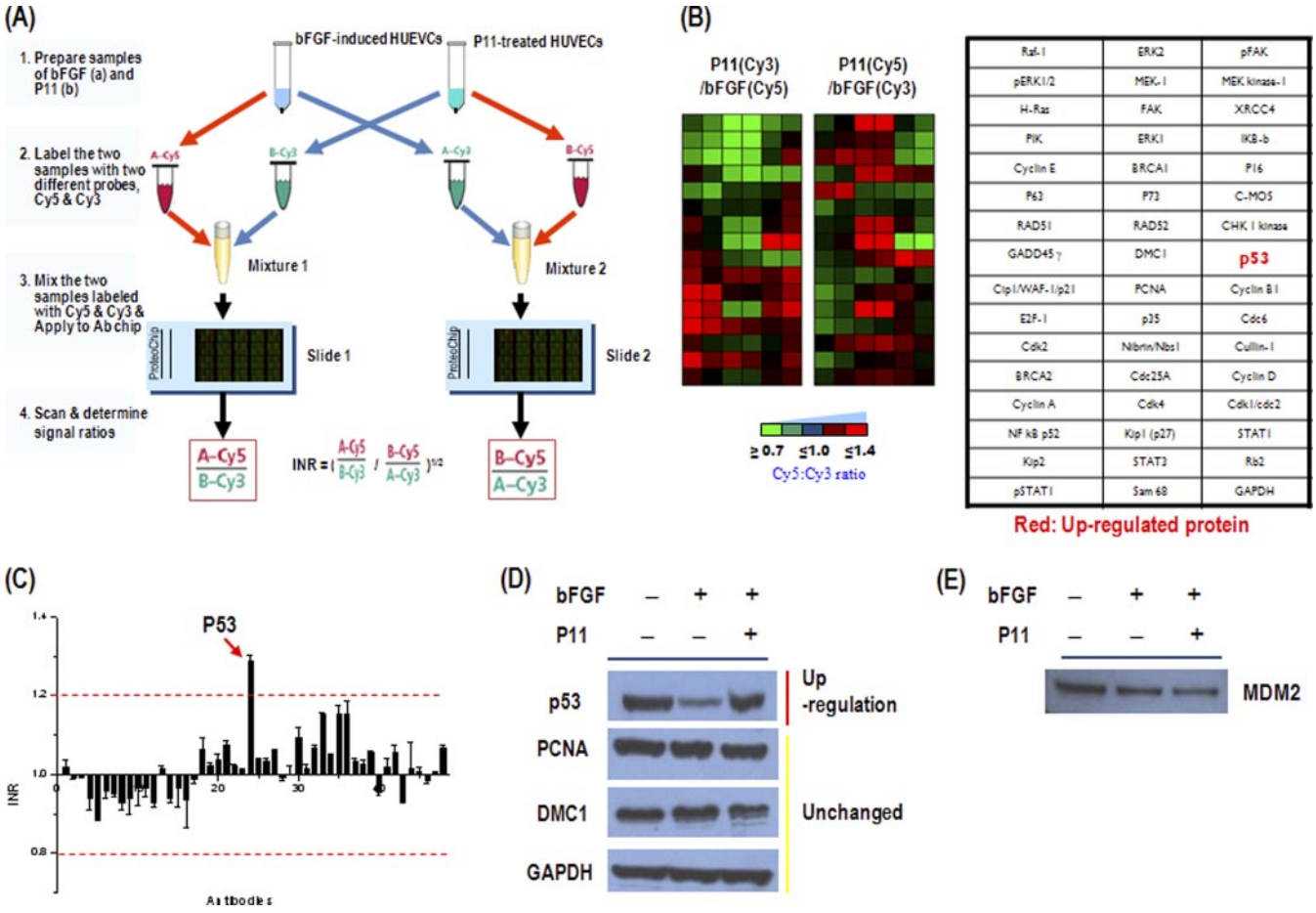

FIG. 2. **Profiling of protein expression in P11-treated HUVECs using antibody microarray.** *A*, Schematic diagram of cell signaling protein expression profiling in P11-treated HUVECs using antibody microarray chip. The labeled samples were concentrated and incubated on antibody array for 1 h at 37 °C. The slides were analyzed using a fluorescence microarray scanner. The tested spots were normalized with the mean values of the Cy5:Cy3 signal ratios of the protein spots using Internally Normalized Ratios (INRs) method. The Cy5/Cy3 values are required to calculate Internally Normalized Ratios (INRs). Proteins were categorized as up-regulated, down-regulated, or unchanged in the test sample compared with the reference sample. *B*, Graded virtual image of Cy5:Cy3 ratios at spots within slides and the antibody map of the antibody array chip. *C*, Graphical representation of Cy5:Cy3 ratios on antibody arrays. Proteins having a normal median ratio in the range of 1.0 were considered as unchanged in expression. Red arrows show up-regulated proteins. *D*, The antibody microarray-based protein expression profile was confirmed by immunoblot analysis. Protein extracts (10–30 mg) were separated on a NuPAGE 4–12% Bis-Tris gel and transferred onto PVDF membranes. After blocking, the membrane was incubated with the indicated primary antibody, washed and then further incubated with HRP-conjugated anti-IgG antibody. Western blots were developed using an ECL system (Santa Cruz Biotechnology) for the detection of signals. *E*, Western blot analysis of MDM2 expression in P11-treated HUVECs.

the colocalization of P11 and the integrin α_v subunit in HUVECs using confocal microscopy. P11-FITC overlapped with integrin α_v on the membrane surface of HUVECs (Fig. 4*B*). We found that P11 uptake by HUVECs was mediated by caveolin and clathrin (Figs. 4*C* and 4*D*). Integrin trafficking also becomes internalization through various coat proteins. Particularly, integrins such as $\alpha_v\beta_1$, $\alpha_v\beta_3$, $\alpha_v\beta_5$, $\alpha_v\beta_8$, and $\alpha_5 b_1$ endocytosis are mediated through clathrin-coated membrane domains in the most part (73). Caveolin is involved in uptake of cholesterol-enriched membrane microdomains which is caused by inhibition of cell adhesion on ECM. A novel pathway in which integrins prevent down-regulation of ERK, PI3K, and Rac-dependent pathways is mediated by inhibiting caveolin-1-dependent endocytosis (77). Therefore, our findings strongly suggest integrin $\alpha_v\beta_3$-dependent penetration of P11 into bFGF-stimulated HUVECs mediated by the actions of caveolin may be closely related with P11-induced weakening of the cell adhesion, resulting p53-induced apoptosis of P11-treated HUVECs. Further attempts were made to examine the mechanism of endocytosis.

Suppression of MAPK (MEK and ERK1/2) Activation and Regulation of Transcription Factors in bFGF-Stimulated HUVECs by P11—Further studies on cellular signaling pathways will be necessary to fully understand the inhibitory mechanism of cell-penetrating P11 on bFGF-induced HUVEC proliferation. To further elucidate the mode of action by which P11 exhibits its antiproliferative effect after internalization into HUVECs, we examined which transcription factors and sig-

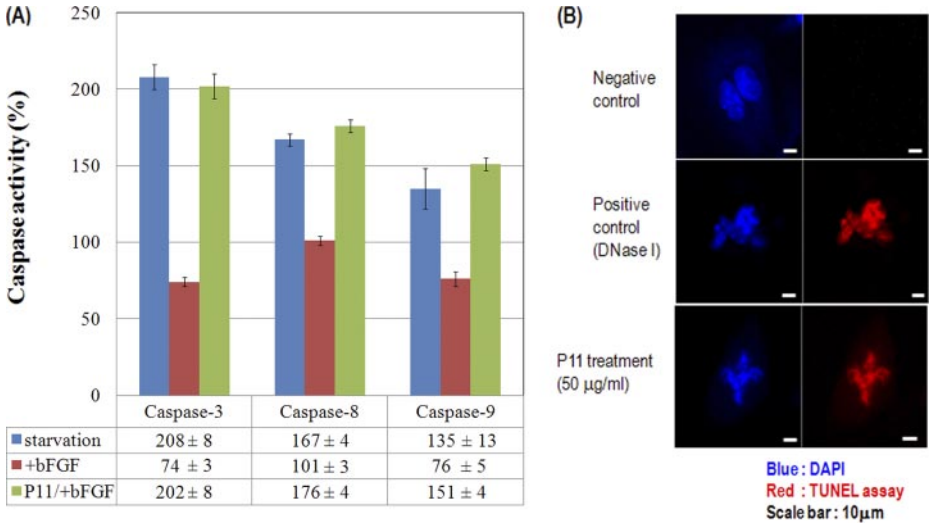

FIG. 3. **Induction of apoptosis in HUVECs treated with P11.** *A*, Activities of caspases-3, -8, and caspase-9 in P11-treated HUVECs. The caspase activities were measured by determining the ability of cell extracts to cleave the colorimetric substrates DEVD-pNA (for caspase-3 activity), IETD-pNA (for caspase-8 activity), and LEHD-pNA (for caspase-9 activity). Comparison of the absorbance of *p*NA from a P11-treated sample with an untreated control allows determination of the fold increase in caspase activity. Results are mean ± S.D. (from four separate experiments). *B*, *In situ* apoptosis TUNEL assay detection of apoptosis in HUVECs treated with P11. We treated bFGF (10 ng/ml) in the presence or absence of P11 (50 μg/ml) in HUEVCs. After overnight incubation, we performed the TUNEL assay as described in *Materials and Methods*. We used the label solution as a negative control and DNase I (50 unit/ml) as a positive control, respectively.

naling proteins involved in cell proliferation are regulated by the internalized peptide. It was reported that bFGF-induced ERK activation was required for vascular angiogenesis (41). Integrin $\alpha_v\beta_3$ antagonist inhibited the ERK signaling lead to endothelial cell apoptosis and blockade of angiogenesis (42). Antagonists of integrin $\alpha_v\beta_3$ disrupt bFGF-induced neovascularization via suppressing c-Raf-ERK activation (43). Thus, we investigated the effect of P11 on the MAPK signaling pathway in bFGF-stimulated HUVECs. Exogenous bFGF induced rapid phosphorylation of ERK1/2 and MEK in HUVECs (Fig. 5*A*). Activation of ERK1/2 was observed as early as 2 min after bFGF treatment, and maximal activation was reached at 5 min. P11 (10 μg/ml) significantly inhibited bFGF-induced phosphorylation of ERK1/2 as early as 5 min and MEK at 5 min. These inhibitory effects were accompanied by suppression of HUVEC migration and proliferation induced by bFGF. U0126, a MEK inhibitor, also prevented the phosphorylation of ERK1/2 and MEK (Fig. 5A), indicating that P11 is blocking the MAPK pathway in HUVECs. Because activation of MAPK (ERK1/2) is reported to induce up-regulation of the c-Fos gene (44, 45), we then tested the activities of several transcription factors such as NF-kB, CREB-1, c-Rel, c-Fos and ATF-2 using lysates of bFGF-induced HUVECs in the presence or absence of P11. A 96-well plate coated with oligomeric probes corresponding to the five transcription factors was incubated with HUVEC lysates, and activities of the transcription factors were determined by sandwich immunoassay. P11 significantly prevented activation of c-Fos and CREB-1 in HUVECs within 1 h after stimulation with bFGF. On the other hand, ATF-2 activity was increased by P11 (Fig. 5*B*). These findings suggest that P11 regulates the activities of transcription factors for the inhibition of HUVEC proliferation. Previous report reveals that sustained activation of ERK by $\alpha_v\beta_3$ ligation during angiogenesis may suppress p53 activity, thereby enhancing endothelial cell survival and maturation of newly sprouting blood vessels (46). Several lines of experimental data demonstrate that MEK and ERK1/2 activation is critical for the stimulation of HUVEC proliferation and that P11-mediated inhibition of endothelial cell proliferation is achieved by regulation of transcription factors including c-Fos via perturbation of ERK1/2 activation related with p53-induced apoptosis.

DISCUSSION

The main purpose of this study was to identify intracellular proteins that are involved in anti-proliferative mechanism of P11 in bFGF-stimulated HUVECs by a pharmacoproteomic analysis such as ProteoChip-based antibody array.

We have demonstrated a wide range of biological applications for antibody-arrayed protein chip technology (47, 48). We performed global analysis of protein expression profiles using high density antibody microarrays, which were constructed on a ProteoChip to analyze the expression patterns of endogenous cell signaling proteins in angiogenin-treated HUVECs (47). Antibody-arrayed protein chip analysis was used to identify the molecular components involved in the reprogramming process of Oct4 and/or Nanog overexpression in NIH 3T3 cells (48). In these reports, a proteomic approach using antibody-based protein array could provide insights into the cellular mechanism of new lead molecules in terms of pharmacoproteomic approach. We used antibody

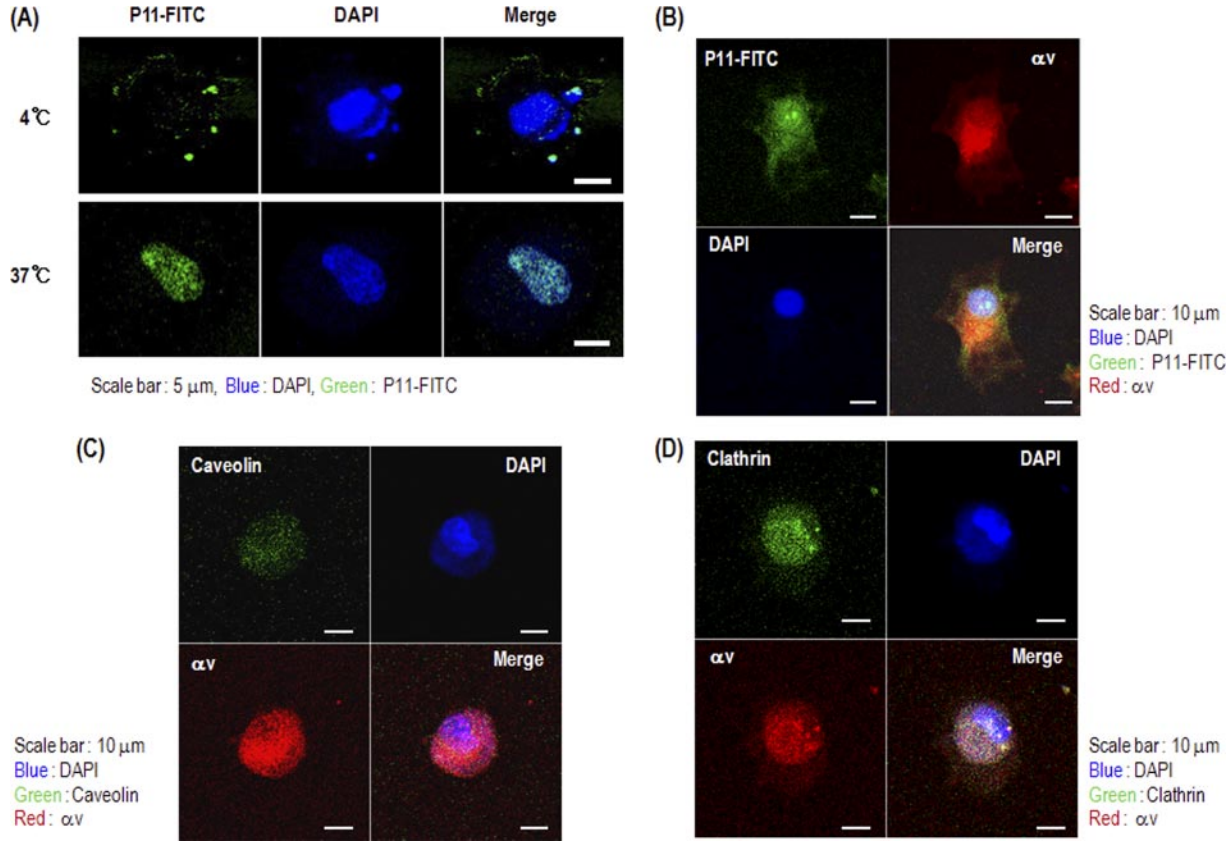

FIG. 4. **Internalization of P11 into HUVEC membranes.** Confocal microscopy of HUVECs (*A*) incubated with P11-FITC was performed to demonstrate internalization of the peptide. The cells were treated with FITC-labeled P11 (1.0 μg/ml) at 4 °C or 37 °C. *B*, HUVECs were treated with FITC-labeled P11(1.0 μg/ml) for 10 min and followed by anti-integrin α_v mAb (10 μg/ml) for 30 min. Secondary antibody labeled with TRITC-phalloidin. The cells were then viewed and photographed by a confocal microscope using a FITC filter. (*C* and *D*) HUVECs were treated with P11 (10 μg/ml) for 10 min, followed by anti-caveolin mAb (10 μg/ml) (*C*) or anti-clathrin mAb (10 μg/ml) (*D*). And then the cells were treated with anti-integrin α_v mAb (10 μg/ml) for 30 min, respectively. Secondary antibodies labeled with FITC or TRITC-phalloidin. The cells were then viewed and photographed by a confocal microscope using a FITC filter.

microarrays fabricated by immobilizing 48 distinct antibodies against cell cycle-related proteins on ProteoChip base plates to examine anti-proliferative effect of P11 through the analysis of the expression pattern of cell signaling proteins in P11-treated HUVECs. And we found that the apoptotic protein expression level of p53 was increased in P11-treated samples (Fig. 2). Our data also show that the expression of MDM2 was down-regulated in P11-treated HUVECs (Fig. 2E). MDM2 is known to be a negative regulator of p53 (24). This result indicates that p53 stability in P11-treated cells is promoted by decreasing MDM2 expression. Further work on how p53 expression was increased by treatment of P11 in bFGF-stimulated HUVECs via integrin $\alpha v\beta 3$-mediated internalization will be remained. Previous findings suggest that integrin $\alpha_v\beta_3$ can promote cell death when unligated, or "ligated" by soluble ligands, both *in vitro* and *in vivo* (51, 52).

Integrin $\alpha_v\beta_3$ is selectively expressed only on angiogenic endothelial cells explains to a large degree the important role in angiogenesis attributed to integrin $\alpha_v\beta_3$ function. Integrin antagonism by endogeneous soluble ligands enhances the activation of caspase 8 (and apoptosis) among ECM-attached endothelial cells in a PKA-dependent manner (40, 51). Antagonists of integrins $\alpha_v\beta_3$ and $\alpha_5\beta_1$ appear to function principally by triggering apoptosis, because pharmacological agents that block apoptosis rescue neovascularization in the presence of integrin antagonists. Considering these results, it becomes clear that mice lacking $\alpha_v\beta_3$ behave as one might expect, given that the endothelial cells in these mice are unresponsive to $\alpha_v\beta_3$ antagonists. Moreover, observations in these mice suggest that the action of endogenous integrin antagonists may play a particularly important role during pathological forms of angiogenesis (52). Cell penetrating peptides such as RGD and endostatin cause apoptosis in endothelial cells through activation of caspases (13, 14). The caspase-9 pathway (the intrinsic pathway of apoptosis) induced by growth factor withdrawal or stresses, is perturbed by integrin ligation, possibly by suppression of p53 activation (53). Antagonists of integrin $\alpha_v\beta_3$ suppress retinal neovascularization in p53wt animals, yet have no antiangiogenic activity in $p53^{-/-}$ animals (23). As p53 is generally assumed to be involved selectively in the regulation of the intrinsic apoptosis pathway, these data implicate caspase 9, rather than caspase 8, in EC apoptosis in

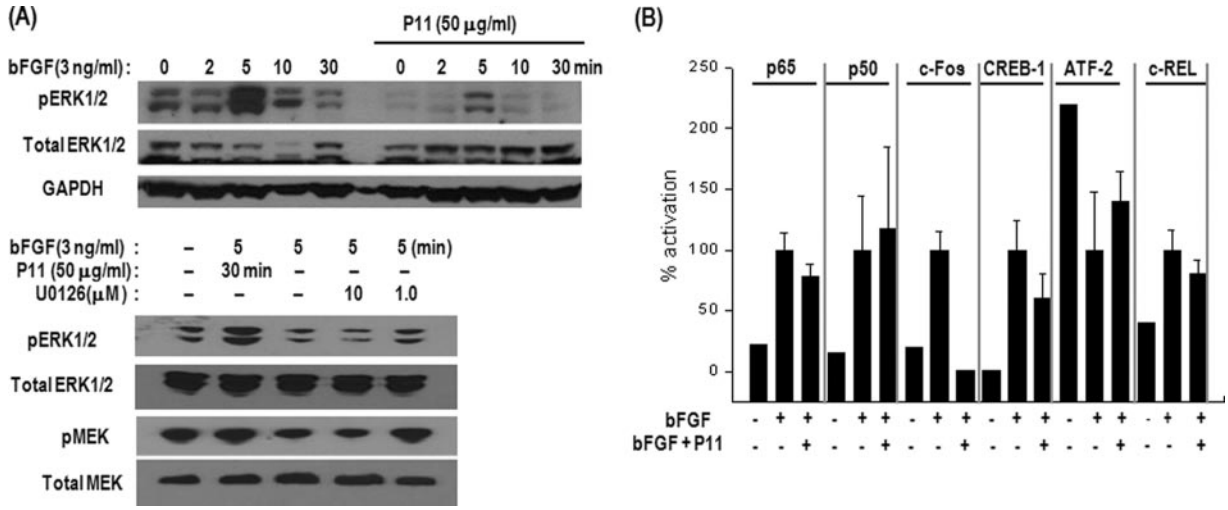

FIG. 5. **Effects of P11 on activities of MAP kinases and transcription factors in bFGF-induced HUVECs.** *A*, HUVECs were preincubated with or without P11 (10 μg/ml, 15 μM) for 30 min and then stimulated with bFGF (3 ng/ml). At the indicated time after bFGF stimulation, the cell lysates were analyzed by Western blotting for the phosphorylation of MEK and ERK1/2. *B*, Activity assay of various transcription factors in bFGF-induced HUVECs treated with or without P11. HUVECs were preincubated with P11 (10 μg/ml) for 30 min, followed by stimulation with bFGF for 30 min. Activation of transcription factors was analyzed using a BD™ TransFactor profiling Kit (Becton Dickinson Science). The histograms represent the relative intensities of the transcription factors activities as determined by colorimetric analyses. The data show the means of three independent experiments (mean ± S.E.).

the retina (42). On the other hand, casepase-8, which plays a role in p53-induced apoptosis, was activated by unligated integrin $\alpha_v\beta_3$ followed by apoptosis (40). Caspase 8 activation can also trigger mitochondrial release of effectors, leading to caspase 9 activation and apoptosis via the "type II" extrinsic pathway. Our data appear that caspaseActivation of caspases-3, -8, and -9 was observed in P11-treated HUVECs induced by bFGF, compared with only bFGF-stimulated HUVECs. In addition, nuclear condensation in P11-treated cells was revealed by TUNEL assay (Fig. 3). These data indicate that caspase-9 and -8 activities are promoted in P11-treated HUVECs and subsequently resulted in downstream activation of caspase-3 via up-regulation of p53. Furthermore, we found that P11 was a potent inhibitor of MEK, ERK1/2 and c-Fos in bFGF-induced HUVECs, resulting in the inhibition of HUVEC proliferation, migration and capillary-like structure formation. These results demonstrate that internalized P11 inhibited the cell proliferation by blocking the MAPK pathway and thus triggering cell apoptosis via increased p53 expression (Figs. 1, 2, 3, and 5). MAP kinases regulate a variety of biological functions by phosphorylating specific target molecules such as transcription factors. Exogenous bFGF stimulates only ERK1/2 activation among the MAPK signaling pathways (Fig. 5*A*). The activation of the ERK1/2 signaling pathway presumably plays a pivotal role in the stimulation of endothelial cell proliferation (41, 54). However, it also protects cells from many forms of apoptosis (55, 56). Activated ERKs regulate a variety of cellular functions that are critical to angiogenesis, including stimulation of migration (57) and formation of tube-like structures (58). In this regard, we found that P11-mediated antiangiogenesis is linked to the deactivation of ERK1/2 signaling in HUVECs. In fact, it was reported that migration of endothelial cells following wounding of the endothelium requires ERK1/2 phosphorylation, because blocking of ERK1/2 activation by the specific MEK inhibitor U0126 prevents bFGF-stimulated ERK activation and subsequently inhibits neovascularization (58, 59). The inhibition of angiogenesis by P11 may be, at least in part, achieved through interference of ERK1/2 activation. Sustained activation of ERK by $\alpha_v\beta_3$ ligation during angiogenesis may suppress p53 activity, thereby enhancing endothelial cell survival and maturation of newly sprouting blood vessels (46). Our experimental data strongly suggest that P11-mediated prevention of HUVEC proliferation is achieved by regulation of transcription factors including c-Fos via perturbation of ERK1/2 activation obtained from P11-induced integrin $\alpha_v\beta_3$ unligation and thereby promoting p53-induced apoptosis. Integrin ligation also leads to the activation of FAK (60). FAK activation occurs upstream of ERK and PI3K, and is likely to account for at least a portion of the ability of integrins to suppress p53-mediated apoptosis. FAK deficient mouse embryos die early (61) and cells derived from $FAK^{-/-}$ mice can only be cultured in a p53-deficient background, despite the fact that these cells still activate ERK and PI3K pathways (60). Interestingly, dominant-negative forms of FAK, such as FRNK, can also either induce apoptosis or predispose cells to apoptosis initiated by other means.

In addition, our study shows that the activity of c-Fos decreased whereas that of ATF-2 slightly increased in P11-treated HUVECs stimulated with bFGF due mainly to the blockade of ERK1/2 activation and subsequent suppression of cell proliferation. It was reported that endothelial cells in

developing vessels exposed to increased VEGF and FGF signaling resulted in excess centrosomes and increased aneuploid via either MEK/ERK or AKT to cyclin E/Cdk2 (62). Therefore, we postulate that MEK and ERK signaling is blocked by P11, and that the resulting disturbance of downstream signaling, *i.e.* deactivation of several transcription factors including c-Fos and CREB in bFGF-stimulated HUVECs, may result in the inhibition of cell proliferation. Clearly, more information is required to understand the full context of angiogenic signaling networks. Because tumor growth requires angiogenesis and P11 inhibits angiogenesis both *in vitro* and *in vivo*, we evaluated the efficacy of P11 as an inhibitor of angiogenesis-dependent tumor growth in a mouse tumor model. It was noteworthy that B16F10 melanoma-induced neovascularization was remarkably prevented by P11 (data not shown). Based on these data, we propose that P11 should be considered as a new angiogenesis inhibitor and novel target for correcting abnormal vasculature. Recently, integrin $\alpha_v\beta_3$ was used as a target for gene therapy of tumors. Hood and colleagues demonstrated that the administration of nanoparticles containing a dominant-negative Raf-1 gene as a vector caused inhibition of tumor progression in tumor-bearing mice (9). Nanoparticles containing an anti-$\alpha_v\beta_3$ antibody (10), and bacteriophage displaying RGD peptide that binds to inetgrin $\alpha_v\beta_3$ (8), were concentrated in the tumor vasculature. Thus, endothelial $\alpha_v\beta_3$ integrin can be used as a target for delivering therapeutic agents such as antibodies, peptide inhibitors and therapeutic genes to tumor blood vessels to increase the effectiveness of tumor treatment and reduce side effects without the complications encountered in chemotherapy. P11 shows selective targeting to integrin $\alpha_v\beta_3$, which has been shown to inhibit cell proliferation by penetrating cells, and thus may have potential in antiangiogenic therapy.

In our previous study, P11, a novel peptide sequence containing Ser-Asp-Val (SDV), was shown to specifically bind to integrin $\alpha_v\beta_3$ instead of the RGD sequence, a common binding motif of the integrin receptor (22). The SDV sequence is a type I PDZ-binding domain (S/T-X-V) that can recognize PSD-95 (63). Further, it was found that the type I PDZ recognition sequence of a cytoplasmic domain of α6a/α5 integrin and a novel sequence in α6B integrin can bind to TIP2/GIPC (64). Our finding was the first demonstration that the type I PDZ-recognition motif can bind to the ligand binding site of integrin $\alpha_v\beta_3$. The PDZ-binding motif-containing P11 peptide was rapidly internalized into HUVECs at 37 °C as early as 5 min (Fig. 4*A*). This internalization process was not a nonspecific penetration as in simple diffusion but was specifically mediated by integrin $\alpha_v\beta_3$ and regulated by temperature (Fig. 4*B*). The role of integrin endocytic cycle is increase in cell adhesion, spreading and regulation of motility. Integrin endo/exocytic cycle has at least 3 types of pathways such as (1) clathrin-mediated endocytosis (2) caveolae-mediated endocytosis, and (3) clathrin-caveolae-independent endocytosis (73). Endostatin is rapidly taken up in murine brain endothelial cells where it undergoes degradation (31). However, the cell entry mechanisms of endostatin and RGD have not yet been elucidated. There are several reports that fibrinogen bound to the surfaces of A549 cells is internalized by endocytosis via RGD-dependent binding to integrin $\alpha_v\beta_3$ (65). Additionally, the internalization and degradation of matrix-bound vitronectin are mediated by integrin $\alpha_v\beta_5$ and involve protein kinase C (66). Integrin $\alpha_v\beta_5$ is internalized in its active, vitronectin-bound form (67, 68) through clathrin-coated pits (69). Adenoviral entry via α_v integrin is dependent on Rab5 and mediated by clathrin (70). Human cytomegalovirus enters cells via clathrin-dependent endocytosis in an integrin $\alpha_v\beta_3$-mediated event (71). The entry of human parechovirus 1 (HPEV-1) into host cells is mediated by a clathrin-dependent pathway (72). Importantly, integrin-mediated endocytic machinery combine with different integrin receptors such as $\alpha_v\beta_1$, $\alpha_v\beta_3$, $\alpha_v\beta_5$, $\alpha_v\beta_8$, and $\alpha_5\beta_1$ and invade into cells by using the route of clathrin (73). P11 peptide is also internalized with clustering through clathrin-mediated endocytosis such as RGD petide. Interestingly, our data using double-labeling experiments show that P11 internalization mediated by integrin $\alpha_v\beta_3$ occurred via both caveolin- and clathrin-dependent endocytotic pathway (Figs. 4*C* and 4*D*). Clathrin-independent and caveolae-mediated internalization of integrins has been described for certain integrins including integrin $\alpha_2\beta_1$. Caveolin-1 is associated with some integrins including $\alpha_v\beta_3$ and $\alpha_5\beta_1$, and integrin $\alpha_2\beta_1$ redistributes to caveolae after integrin clustering (76). β 1 integrins play an important role in the process of endocytosis of fibronectin and fibronectin matrix fibrils by caveolin-mediated event (75). Recent report demonstrated that caveolin plays critical role in rapid internalization of cholesterol-enriched membrane microdomains, when cells are detached from ECM. In this process, integrin-mediated regulation of ERK, phosphatidylinositol-3-OH kinase (PI3K) and Rac pathways is dependent on caveolin-1. Inhibition of caveolin-1-dependent endocytosis results in preventing down-regulation of ERK, PI3K, and Rac-dependent pathways induced by cell detachment (77). These reports strongly support our finding that cell penetration by P11 can occur through integrin $\alpha_v\beta_3$-mediated endocytosis dependent on caveolin and this event might be caused by perturbing the cell attachment.

In summary, using a comparative pharmacoproteomic analysis of cellular signaling proteins in P11-treated HUVECs, we have investigated the antiproliferative mechanism of P11, a novel cell-permeable antiangiogenic peptide containing type I PDZ-binding motif, which specifically recognizes integrin $\alpha_v\beta_3$ on the cell surface via up-regulation of p53 in the cells. Additional analyses were supported to demonstrate the proteomic result of P11-induced up-regulation of p53. Further works are required to elucidate how p53 expression was increased by treatment of P11 in bFGF-stimulated HUVECs. Taken together, these data strongly suggest that the pharmacoproteomic approach using antibody-arrayed ProteoChip may be

a valuable tool for understanding of selective molecular mechanism of new drugs.

* This work was supported by Korea Biotech R&D Group of Next-generation growth engine project of the Ministry of Education, Science and Technology, Republic of Korea (2010K001236).

¶¶ To whom correspondence should be addressed: Hoseo University, Asan 336-795, Korea. Tel.: +82-41-540-5974; Fax: +82-41-532-4404; E-mail: ickang@hoseo.edu.

REFERENCES

1. Folkman J. in Biology of Endothelial Cells. eds. Jaffe, E. A. (1984) (Martinus Nijhoff, The Hague, The Netherlands), 413–428
2. Blood, C. H., and Zetter, B. R. (1990) Tumor interactions with the vasculature: angiogenesis and tumor metastasis. *Biochim. Biophys. Acta* **1032,** 89–118
3. Fett, J. W., Strydom, D. J., Lobb, R. R., Alderman, E. M., Bethune, J. L., Riordan, J. F., and Vallee, B. L. (1985) Isolation and characterization of angiogenin, an angiogenic protein from human carcinoma cells. *Biochemistry* **24,** 5480–5486
4. Varner, J. A., Brooks, P. C., and Cheresh, D. A. (1995) Review: the integrin $\alpha_v\beta_3$: angiogenesis and apoptosis. *Cell Adhes Commun* **3,** 367–374
5. Brooks, P. C., Clark, R. A., and Cheresh, D. A. (1994) Requirement of vascular integrin $\alpha_v\beta_3$ for angiogenesis. *Science* **264,** 569–571
6. Brooks, P. C., Strömblad, S., Klemke, R., Visscher, D., Sarkar, F. H., and Cheresh, D. A. (1995) Antiintegrin $\alpha_v\beta_3$ blocks human breast cancer growth and angiogenesis in human skin. *J. Clin. Invest.* **96,** 1815–1822
7. Ruoslahti, E. (2002) Antiangiogenics meet nanotechnology. *Cancer Cell* **2,** 97–98
8. Arap, W., Pasqualini, R., and Ruoslahti, E. (1998) Cancer treatment by targeted drug delivery to tumor vasculature in a mouse model. *Science* **279,** 377–380
9. Hood, J. D., Bednarski, M., Frausto, R., Guccione, S., Reisfeld, R. A., Xiang, R., and Cheresh, D. A. (2002) Tumor regression by targeted gene delivery to the neovasculature. *Science* **296,** 2404–2407
10. Sipkins, D. A., Cheresh, D. A., Kazemi, M. R., Nevin, L. M., Bednarski, M. D., and Li, K. C. P. (1998) Detection of tumor angiogenesis in vivo by alphaVbeta3-targeted magnetic resonance imaging. *Nat Med* **4,** 623–626
11. Cheresh, D. A. (1991) Structure, function and biological properties of integrin $\alpha_v\beta_3$ on human melanoma cells. *Cancer Metastasis Rev* **10,** 3–10
12. Friedlander, M., Theesfeld, C. L., Sugita, M., Fruttiger, M., Thomas, M. A., Chang, S., and Cheresh, D. A. (1996) Involvement of integrins alpha v beta 3 and alpha v beta 5 in ocular neovascular diseases. *Proc. Natl. Acad. Sci. U.S.A.* **93,** 9764–9769
13. Buckley, C. D., Pilling, D., Henriquez, N. V., Parsonage, G., Threlfall, K., Scheel-Toellner, D., Simmons, D. L., Akbar, A. N., Lord, J. M., and Salmon, M. (1999) RGD peptides induce apoptosis by direct caspase-3 activation. *Nature* **397,** 534–539
14. Aguzzi, M. S., Giampietri, C., De, Marchis, F., Padula, F., Gaeta, R., Ragone, G., Capogrossi, M. C., and Facchiano, A. (2004) RGDS peptide induces caspase 8 and caspase 9 activation in human endothelial cells. *Blood* **103,** 4180–4187
15. Humphries, M. J., Olden, K., and Yamada, K. M. (1986) A synthetic peptide from fibronectin inhibits experimental metastasis of murine melanoma cells. *Science* **233,** 467–470
16. Brooks, P. C., Montgomery, A. M., Rosenfeld, M., Reisfeld, R. A., Hu, T., Klier, G., and Cheresh, D. A. (1994) Integrin alpha v beta 3 antagonists promote tumor regression by inducing apoptosis of angiogenic blood vessels. *Cell* **79,** 1157–1164
17. Ferguson, T. A., Mizutani, H., and Kupper, T. S. (1991) Two integrin-binding peptides abrogate T cell-mediated immune responses in vivo. *Proc. Natl. Acad. Sci. U.S.A.* **88,** 8072–8076
18. Maeshima, Y., Colorado, P. C., and Kalluri, R. (2000) Two RGD-independent $\alpha_v\beta_3$ integrin binding sites on tumstatin regulate distinct anti-tumor properties. *J. Biol. Chem.* **275,** 23745–23750
19. Huang, J., and Kontos, C. D. (2002) PTEN modulates vascular endothelial growth factor mediated signaling and angiogenic effects. *J. Biol. Chem.* **277,** 10760–10766
20. Nguyen, M., Shing, Y., and Folkman, J. (1994) Quantitation of angiogenesis and antiangiogenesis in the chick embryo chorioallantoic membrane. *Microvasc Res* **47,** 31–40
21. Lee, Y., Kang, D. K., Chang, S. I., Han, M. H., and Kang, I. C. (2004) High-throughput screening of novel antagonistic peptides against integrin $\alpha v\beta 3$ from hexapeptide library by using protein microarray. *J Biomol Screen* **9,** 687–694
22. Choi, Y., Kim, E., Lee, Y., Han, M. H., and Kang, I. C. (2010) Site-specific inhibition of integrin $\alpha_v\beta_3$-vitronectin association by a ser-asp-val sequence through an Arg-Gly-Asp-binding site of the integrin. *Proteomics* **10,** 72–80
23. Stromblad, S., Fotedar, A., Brickner, H., Theesfeld, C., Aguilar, de Diaz E., Friedlander, M., and Cheresh, D. A. (2002) Loss of p53 compensates for av-integrin function in retinal neovascularization, *J. Biol. Chem.* **277,** 13371–13374
24. Haupt, Y., Maya, R., Kazaz, A., and Oren, M. (1997) MDM2 promotes the rapid degradation of p53. *Nature* **387,** 296–299
25. Bottger, A., Bottger, V., Sparks, A., Liu, W. L., Howard, S. F., and Lane, D. P. (1997) Design of a synthetic MDM2-binding mini protein that activates the p53 response in vivo. *Curr. Biol.* **7,** 860–869
26. Kubbutat, M. H., and Vousden, K. H. (1997) Proteolytic cleavage of human p53 by calpain: a potential regulator of protein stability. *Mol. Cell. Biol.* **17,** 460–468
27. Maki, C. G. (1999) Oligomerization is required for p53 to be efficiently ubiquitinated by MDM2. *J. Biol. Chem.* **274,** 16531–16535
28. Shirangi, T. R., Zaika, A., and Moll, U. M. (2002) Nuclear degradation of p53 occurs during down-regulation of the p53 response after DNA damage. *FASEB J.* **16,** 420–422
29. Moll, U. M., and Petrenko, O. (2003) The MDM2-p53 Interaction. *Molecular Cancer Research* **1,** 1001–1008
30. Sudhakar, A., Sugimoto, H., Yang, C., Lively, J., Zeisberg, M., and Kalluri, R. (2003) Human tumstatin and human endostatin exhibit distinct antiangiogenic activities mediated by $\alpha_v\beta_3$ and $\alpha_5\beta_1$ integrins. *Proc. Natl. Acad. Sci. U.S.A.* **100,** 4766–4771
31. Dhanabal M. (1999) Endostatin Induces Endothelial Cell Apoptosis. *J. Biol. Chem.* **274,** 11721–11726
32. Dixelius, J., Larsson, H., Sasaki, T., Holmqvist, K., Lu, L., Engström, A., Timpl, R., Welsh, M., and Claesson-Welsh, L. (2000) Endostatin-induced tyrosine kinase signaling through the Shb adaptor protein regulates endothelial cell apoptosis. *Blood* **95,** 3403–3411
33. Wickström, S. A., Alitalo, K., and Keski-Oja, J. (2002) Endostatin associates with integrin alpha5beta1 and caveolin-1, and activates Src via a tyrosyl phosphatase-dependent pathway in human endothelial cells. *Cancer Research* **62,** 5580–5589
34. Kim, Y. M., Hwang, S., Kim, Y. M., Pyun, B. J., Kim, T. Y., Lee, S. T., Gho, Y. S., and Kwon, Y. G. (2002) Endostatin blocks vascular endothelial growth factor-mediated signaling via direct interaction with KDR/Flk-1. *J. Biol. Chem.* **277,** 27872–27879
35. Colorado, P. C., Torre, A., Kamphaus, G., Maeshima, Y., Hopfer, H., Takahashi, K., Volk, R., Zamborsky, E. D., Herman, S., Sarkar, P. K., Ericksen, M. B., Dhanabal, M., Simons, M., Post, M., Kufe, D. W., Weichselbaum, R. R., Sukhatme, V. P., and Kalluri, R. (2000) Anti-angiogenic Cues from Vascular Basement Membrane Collagen. *Cancer Research* **60,** 2520–2526
36. Sudhakar, A., Nyberg, P., Keshamouni, V. G., Mannam, A. P., Li, J., Sugimoto, H., Cosgrove, D., and Kalluri, R. (2005) Human $\alpha 1$ type IV collagen NC1 domain exhibits distinct antiangiogenic activity mediated by $\alpha 1\beta 1$ integrin. *J. Clin. Invest.* **115,** 2801–2810
37. Kamphaus, G. D., Colorado, P. C., Panka, D. J., Hopfer, H., Ramchandran, R., Torre, A., Maeshima, Y., Mier, J. W., Sukhatme, V. P., and Kalluri, R. (2000) Canstatin, a Novel Matrix-derived Inhibitor of Angiogenesis and Tumor Growth. *J. Biol. Chem.* **275,** 1209–1215
38. Panka, D. J., and Mier, J. W. (2003) Canstatin Inhibits Akt Activation and Induces Fas-dependent Apoptosis in Endothelial Cells. *J. Biol. Chem.* **278,** 37632–37636
39. Magnon, C., Galaup, A., Mullan, B., Rouffiac, V., Bouquet, C., Bidart, J. M., Griscelli, F., Opolon, P., and Perricaudet, M. (2005) Canstatin acts on endothelial and tumor cells via mitochondrial damage initiated through interaction with alphavbeta3 and alphavbeta5 integrins. *Cancer Research* **65,** 4353–4361
40. Stupack, D. G., Puente, X. S., Boutsaboualoy, S., Storgard, C. M., and Cheresh, D. A. (2001) Apoptosis of adherent cells by recruitment of

caspase-8 to unligated integrins. *J. Cell Biol.* **155,** 459–470
41. Eliceiri, B. P., Klemke, R., Strömblad, S., and Cheresh, D. A. (1998) Integrin $\alpha_v\beta_3$ requirement for sustained mitogen-activated protein kinase activity during angiogenesis. *J. Cell Biol.* **140,** 1255–1263
42. Stupack, D. G., and Cheresh, D. A. (2003) Apoptotic cues from the extracellular matrix: regulators of angiogenesis. *Oncogene* **22,** 9022–9029
43. Hood, J. D., Frausto, R., Kiosses, W. B., Schwartz, M. A., and Cheresh, D. A. (2003) Differential αv integrin-mediated Ras-ERK signaling during two pathways of angiogenesis. *J. Cell Biol.* **162,** 933–943
44. Jalali, S., Li, Y. S., Sotoudeh, M., Yuan, S., Li, S., Chien, S., and Shyy, J. Y. (1998) Shear stress activates p60^{src}-Ras-MAPK signaling pathways in vascular endothelial cells. Arterioscler. *Thromb Vasc Biol* **18,** 227–234
45. Huttunen, P., Hyypiä, T., Vihinen, P., Nissinen, L., and Heino, J. (1998) Echovirus 1 infection induces both stress- and growth-activated mitogen-activated protein kinase pathways and regulates the transcription of cellular immediate-early genes. *Virology* **250,** 85–93
46. Milne, D. M., Campbell, D. G., Caudwell, F. B., and Meek, D. W. (1994) Phosphorylation of the tumor suppressor protein p53 by mitogen-activated protein kinase. *J. Biol. Chem.* **269,** 9253–9260
47. Ahn, E. H., Kang, D. K., Chang, S. I., Kang, C. S., Han, M. H., and Kang, I. C. (2006) Profiling of Differential Protein Expression in angiogenin-Induced HUVECs using Antibody-Arrayed ProteoChip. *Proteomics* **6,** 1104–1109
48. Ajjappala, B. S., Kim, M. S., Kim, E. Y., Kim, J. H., Kang, I. C., and Baek, K. H. (2009) Protein chip analysis of pluripotency-associated proteins in NIH3T3 fibroblast. *Proteomics* **9,** 3968–3978
49. Brooks, P. C., Montgomery, A. M., Rosenfeld, M., Reisfeld, R. A., Hu, T., Klier, G., and Cheresh, D. A. (1994) Integrin alpha v beta 3 antagonists promote tumor regression by inducing apoptosis of angiogenic blood vessels. *Cell* **79,** 1157–1164
50. Brassard, D. L., Maxwell, E., Malkowski, M., Nagabhushan, T. L., Kumar, C. C., and Armstrong, L. (1999) Integrin alpha(v)beta(3)-mediated activation of apoptosis. *Exp. Cell Res.* **251,** 33–45
51. Kim, S., Bakre, M., Yin, H., and Varner, J. A. (2002) Inhibition of endothelial cell survival and angiogenesis by protein kinase A. *J Clin Investig* **110,** 933–941
52. Reynolds, L. E., Wyder, L., Lively, J. C., Taverna, D., Robinson, S. D., Huang, X., Sheppard, D., Hynes, R. O., and Hodivala-Dilke, K. M. (2002) Enhanced pathological angiogenesis in mice lacking beta3 integrin or beta3 and beta5 integrins. *Nat Med* **8,** 27–34
53. Strömblad, S., Becker, J. C., Yebra, M., Brooks, P. C., and Cheresh, D. A. (1996) Suppression of p53 activity and p21WAF1/CIP1 expression by vascular cell integrin alphaVbeta3 during angiogenesis. *J Clin Investig* **98,** 426–433
54. Nakao, S., Kuwano, T., Ishibashi, T., Kuwano, M., and Ono, M. (2003) Synergistic Effect of TNF-α in Soluble VCAM-1-Induced Angiogenesis Through α_4 Integrins. *J. Immunol.* **170,** 5704–5711
55. Cho, S. Y., and Klemke, R. L. (2000) Extracellular-regulated kinase activation and CAS/Crk coupling regulate cell migration and suppress apoptosis during invasion of the extracellular matrix. *J. Cell Biol.* **149,** 223–236
56. Howe, A. K., Aplin, A. E., and Juliano, R. L. (2002) Anchorage-dependent ERK signaling–mechanisms and consequences. *Curr. Opin. Genet. Dev.* **12,** 30–35
57. Klemke, R. L., Cai, S., Giannini, A. L., Gallagher, P. J., de Lanerolle, P., and Cheresh, D. A. (1997) Regulation of cell motility by mitogen-activated protein kinase. *J. Cell Biol.* **137,** 481–492
58. Maru, Y., Yamaguchi, S., Takahashi, T., Ueno, H., and Shibuya, M. (1998) Virally activated Ras cooperates with integrin to induce tubulogenesis in sinusoidal endothelial cell lines. *J. Cell. Physiol.* **176,** 223–234
59. Pintucci, G., Steinberg, B. M., Seghezzi, G., Yun, J., Apazidis, A., Baumann, F. G., Grossi, E. A., Colvin, S. B., Mignatti, P., and Galloway, A. C. (1999) Mechanical endothelial damage results in basic fibroblast growth factor-mediated activation of extracellular signal-regulated kinases. *Surgery* **126,** 422–427
60. Schlaepfer, D. D., Hauck, C. R., and Sieg, D. J. (1999) Signaling through focal adhesion kinase. *Prog Biophys Mol Biol* **71,** 435–478
61. Ilić, D., Furuta, Y., Kanazawa, S., Takeda, N., Sobue, K., Nakatsuji, N., Nomura, S., Fujimoto, J., Okada, M., and Yamamoto, T. (1995) Reduced cell motility and enhanced focal adhesion contact formation in cells from FAK-deficient mice. *Nature* **377,** 539–544
62. Tani, T. T., and Mercurio, A. M. (2001) PDZ Interaction Sites in Integrin α Subunits. *J. Biol. Chem.* **276,** 36535–36542
63. Pintucci, G., Moscatelli, D., Saponara, F., Biernacki, P. R., Baumann, F. G., Bizekis, C., Galloway, A. C., Basilico, C., and Mignatti, P. (2002) Lack of ERK activation and cell migration in FGF-2-deficient endothelial cells. *FASEB J.* **16,** 598–600
64. Fanning, A. S., and Anderson, J. M. (1996) Protein–protein interactions: PDZ domain networks. *Current Biology* **6,** 1385–1388
65. Odrljin, T. M., Haidaris, C. G., Lerner, N. B., and Simpson-Haidaris, P. J. (2001) Integrin alphavbeta3-mediated endocytosis of immobilized fibrinogen by A549 lung alveolar epithelial cells. *Am. J. Respir. Cell Mol. Biol.* **24,** 12–21
66. Panetti, T. S., Wilcox, S. A., Horzempa, C., and McKeown-Longo, P. J. (1995) Alpha v beta 5 integrin receptor-mediated endocytosis of vitronectin is protein kinase C-dependent. *J. Biol. Chem.* **270,** 18593–18597
67. Panetti, T. S., and McKeown-Longo, P. J. (1993) The alpha v beta 5 integrin receptor regulates receptor-mediated endocytosis of vitronectin. *J. Biol. Chem.* **268,** 11492–11495
68. Panetti, T. S., and McKeown-Longo, P. J. (1993) Receptor-mediated endocytosis of vitronectin is regulated by its conformational state. *J. Biol. Chem.* **268,** 11988–11993
69. Memmo, L. M., and McKeown-Longo, P. (1998) The alphavbeta5 integrin functions as an endocytic receptor for vitronectin. *J. Cell Sci.* **111,** 425–433
70. Rauma, T., Tuukkanen, J., Bergelson, J. M., Denning, G., and Hautala, T. (1999) Rab5 GTPase regulates adenovirus endocytosis. *J. Virol.* **73,** 9664–9668
71. Wang, X., Huang, D. Y., Huong, S. M., and Huang, E. S. (2005) Integrin alphavbeta3 is a coreceptor for human cytomegalovirus. *Nat Med* **11,** 515–521
72. Joki-Korpela, P., Marjomäki, V., Krogerus, C., Heino, J., and Hyypiä, T. (2001) Entry of Human parechovirus 1. *J. Virol.* **75,** 1958–1967
73. Pellinen, T., and Ivaska, J. (2006) Integrin traffic. *J. Cell Sci.* **119(Pt18),** 3723–3731
74. Ning, Y., Buranda, T., and Hudson, L. G. (2007) Activated epidermal growth factor receptor induces integrin α2 internalization via caveolae/raft-dependent endocytic pathway. *J. Biol. Chem.* **282,** 6380–6387
75. Shi, F., and Sottile, J. (2008) Caveolin-1-dependent beta1 integrin endocytosis is a critical regulator of fibronectin turnover. *J. Cell Sci.* **121(Pt 14),** 2360–2371
76. Upla, P., Marjomäki, V., Kankaanpää, P., Ivaska, J., Hyypiä, T., Van Der Goot, F. G., and Heino, J. (2004) Clustering induces a lateral redistribution of alpha 2 beta 1 integrin from membrane rafts to caveolae and subsequent protein kinase C-dependent internalization. *Mol. Biol. Cell* **15,** 625–636
77. Echarri, A., and Del Pozo M. A. (2006) Caveolae internalization regulates integrin-dependent signaling pathways. *Cell cycle* **5,** 2179–2182